metals

MDPI

Article

Pyrometallurgical Extraction of Technology and Base Metals from Copper Smelting Slags

Xolisa Camagu Goso [1,*], Kgothatso Gerald Sethosa [1], Alain Nyembwe [2], Kgomotso Charlotte Maluleke [3] and Michel Kalenga [4]

[1] Pyrometallurgy Division, Mintek, 200 Malibongwe Drive, Randburg, Johannesburg 2125, South Africa; kgothatsos@mintek.co.za
[2] School of Chemical and Metallurgical Engineering, University of the Witwatersrand, 1 Jan Smuts Avenue, Braamfontein, Johannesburg 2000, South Africa; alain.nyembwe1@wits.ac.za
[3] Tenova Pyromet, Tenova South Africa (Pty) Ltd., Unit H3-1-004, Midpoint, 162 Tonetti Street, Halfway House, Midrand, Johannesburg 1685, South Africa; kgomotso.maluleke@tenova.com
[4] Department of Metallurgy, University of Johannesburg, Maropeng Building, Doornfontein Campus, 55 Beit Street, Doornfontein, Johannesburg 2094, South Africa; michelk@uj.ac.za
* Correspondence: xolisag@mintek.co.za; Tel.: +27-11-709-4748

Abstract

Copper (Cu) smelting slags are considered secondary reserves of technology metals (TMs) and base metals (BMs), which are crucial for the transition to renewable energy and mechatronic applications. In this study, thermochemical and experimental analyses were conducted to investigate the pyrometallurgical extraction of TMs and BMs from Cu smelting slag. FactSage thermochemical simulations and smelting experiments were carried out at temperatures from 1300 to 1600 °C and with carbon (reductant) additions of 2% to 10% relative to the mass of the feed slag. The results showed that during smelting, gallium (Ga), germanium (Ge), cobalt (Co), and copper (Cu) deported into the iron-based alloy product. Zinc (Zn) and lead (Pb) oxidised to ZnO and PbO, respectively, which were subsequently collected as fumes. The produced alloy mass was more sensitive to carbon addition than to smelting temperature variation. The TM and BM contents in the alloy decreased with increasing carbon addition in the feed; this was attributed to dilution by Fe, Si, and C from the increasing reduction of iron and silicon oxides in the feed slag and dissolution of C in the alloy. High recovery degrees of TMs and BMs in the alloy stream—over 90% for Co and Cu, over 50% for Ga, and over 70% for Ge—were achieved when smelting at 1500 °C with 4% carbon addition. The final alloy comprised 70.5% Fe, 6.6% Co, 23.6% Cu, 0.11% Ga, and 0.13% Ge. The fumes primarily comprised ZnO and, to a lesser extent, PbO, with recovery degrees over 90% for Zn and Pb. These alloy and fume products would be processed following conventional hydrometallurgical separation and purification processes to produce high-purity metals. The pyrometallurgical extraction of TMs and BMs presents an opportunity for the valorisation of Cu smelting slag dumps, especially in Southern Africa, aiming to attain zero-waste industrial processes.

Keywords: Cu slag; FactSage; reduction smelting; gallium; germanium; cobalt

Check for updates

Academic Editor: Corby G. Anderson

Received: 19 January 2026
Revised: 11 March 2026
Accepted: 16 March 2026
Published: 2 April 2026

Copyright: © 2026 by the authors. Licensee MDPI, Basel, Switzerland. This article is an open access article distributed under the terms and conditions of the Creative Commons Attribution (CC BY) license.

1. Introduction

Copper (Cu) is usually found in nature in polymetallic oxidic and sulfidic mineral ores. These mineral deposits are distributed across almost all continents [1]. In Africa, Cu deposits are found in many regions and countries, including the renowned Copperbelt

region, spanning the Democratic Republic of the Congo (DRC) and Zambia, as well as in Namibia and South Africa [2,3]. Sulfidic Cu ores are typically treated through a multistage process involving mining and concentration of low-grade ores, followed by smelting and refining to produce high-purity Cu metal products, mostly Cu cathodes [4,5]. Every tonne of Cu metal produced is estimated to generate 2.2–3 tonnes of Cu slag. The produced mass ratios of Cu metal and slag vary among operations, depending on the characteristics of the mineral ore and the smelting technology used. In 2024, global Cu production was about 22.9 million tonnes, with the amount of corresponding Cu slag estimated at 48 million tonnes [6].

Cu slag dumps, estimated to be in the millions of tonnes in some Southern African countries [2,3], are an environmental nuisance because they typically contain heavy and toxic elements [7–9]. However, Cu slags, especially those produced in Southern Africa, also contain appreciable contents of technology metals (TMs), such as Ga and Ge, and base metals (BMs), such as Cu, Co, Pb, and Zn [10,11].

As Cu slags primarily comprise a fayalitic silicate matrix, magnetite, and spinel-group oxides, matte or sulfide droplets that host residual chalcophile metals are generally entrapped within the slag matrix. Cu, Ni, and Co commonly occur in entrained sulfide/matte droplets or as oxides dissolved in the silicate and/or spinel phases. Zn is also incorporated into silicate or Zn-rich spinels, whereas Pb tends to partition into the glassy matrix or form dispersed Pb-silicate/oxide domains due to its volatility and incompatibility with major crystalline phases [8,12]. Ga and Ge, both lithophiles and highly incompatible at smelting temperatures, are typically enriched in the silicate glass, where they occupy tetrahedral sites or remain as dispersed trace components [8]. The distribution of Cu, Ni, Co, Zn, Pb, Ga, and Ge within smelting slags reflects the combined influences of the melt composition, oxygen partial pressure (pO_2), cooling rate, and efficiency of the slag–matte separation in the primary smelting process.

These TMs and BMs, together with their alloys and compounds, find important applications in modern society, including in the technology sector. Although not classified as 'critical' in some regions, Cu is considered a strategic resource due to its essential role in electrical infrastructure, renewable energy systems, and electrification, combined with declining ore grades and slow development of new mines. Ni and Cu are considered critical metals due to their crucial role in battery technologies and low-carbon energy systems, and their supply is generally concentrated in regions facing geopolitical or environmental challenges. Zn's criticality is moderate, but it is increased by the increased demand for Zn-derived by-products, such as Ge. Pb has low criticality due to its stable supply and recyclability, but environmental regulations and the capacity of ageing mines raise long-term concerns [13,14].

Due to their important industrial applications and supply vulnerabilities, TMs such as Ga and Ge are included in the European Commission's list of critical raw materials [10,14]. Both elements are predominantly recovered as by-products—Ga from bauxite/aluminium processing and Ge from zinc refining; as a result, their production cannot expand in response to demand, as their supply depends on the demand for the primary product. Ga is crucial for high-performance semiconductors such as GaAs and GaN used in light-emitting diodes (LEDs), 5G/6G components, and power electronics, while Ge is essential for fibre-optic systems, infrared optics, high-efficiency solar cells, and advanced semiconductor devices. GaAs is traditionally used as a solar cell. Supply risks are heightened by the geopolitical concentration of refining capacity, making both metals susceptible to export restrictions and trade disruptions. Ga and Ge consistently rank as high-risk materials in criticality assessments, emphasising the need for diversified supply, increased recycling, and alternative sources such as metallurgical residues and slags and end-of-life electronics [14].

Global initiatives for managing the huge amounts of by-product slags include recycling, metal recovery, generation of value-added products, and disposal in slag dumps [15]. Extensive research has investigated extractive metallurgical processes for the metals of interest from Cu slags [16–21]. Most studies have been based on hydrometallurgy, mainly using sulfuric acid as the lixiviant [16,18,19]. In Cu fayalitic slag, sulfuric acid leaching has shown less selectivity for the target metals and high reagent consumption due to co-leaching of Si and Fe. The conventional sulfuric acid lixiviant is then combined with oxidants such as potassium dichromate and sodium chlorate to improve the extraction efficiency and selectivity for Co and Cu, and sometimes Ni and Zn [20,22,23]. However, improvements in the selective and optimal extraction of all the TMs and BMs from Cu slags have not been reported.

The pyrometallurgy route has proven to be practical for recovering TMs and BMs from Cu slags [24–28]. The process involves using carbon and/or hydrogen for the thermal reduction in metal oxides dissolved in the molten Cu slag. Most reduced metals coalesce and settle to form an iron-enriched alloy at the bottom of the containing vessel. With the addition of calcium oxide as a flux, the slag shifts from a primary fayalite composition to a calcium silicate composition. Though the extraction of some metallic elements from Cu slag has been comprehensively studied, the extraction of Co, Ga, and Ge has received limited research attention in the open literature.

Equilibrium operating conditions play a significant role in recovering metals from iron silicate slag in an iron-rich alloy [24–26]. Elements such as Ge preferentially partition from the slag into the iron-rich alloy in highly reducing environments (10^{-6}–10^{-8} atm pO_2). Ga retention in the slag increases with rising temperature. Hwang et al. (2018) demonstrated that Cu recovery in an iron-rich alloy could be enhanced from 11% to 87% by increasing the temperature from 1400 to 1600 °C, using activated carbon as a reductant. Attah-Kyei et al. (2024) reported that high temperatures promote the formation of CO through the Boudouard reaction, which enhances the reduction in Fe, Co, and Ni. The addition of basic fluxing agents—such as CaO, $CaCO_3$, and MgO—facilitates the release of BMs from the slag, with the most pronounced effects observed during the initial stages of the process [24,27]. These fluxes disrupt the silicate network, promoting the formation of silicate tetrahedra and free iron oxides within the molten slag. Zhang et al. (2022) reported high Cu, Fe, Pb, and Zn recoveries from Cu slag at 1450 °C and a slag basicity of 1.2 for a reductant-to-slag ratio of 0.225. In addition, Cu and Mo were successfully extracted from Chilean Cu slag through oxidative and reductive roasting and smelting. The smelting test results of this investigation suggested that the low Cu and Mo contents in the slag could be collected in an iron-rich alloy [29,30].

The objective of the current study was to explore the use of the pyrometallurgical approach to process Southern African Cu slags for the extraction of TMs and BMs. Cu smelting slag was subjected to carbothermic smelting in the presence of graphite to collect Ga, Ge, Cu, and Co in an iron-rich alloy, while Zn and Pb were collected as fumes.

Thermochemical Considerations

Carbothermic smelting of Cu slag can result in the reduction in technology and base metal oxides. At high temperatures > 800 °C, the Boudouard reaction promotes the formation of CO, which is primarily responsible for the reduction in TMs and BMs and their deportment to the alloy [24–27]. In Cu slag, metal oxide reduction, as described in chemical reactions (1)–(10), can occur via a direct or an indirect route and can be predicted using FactSage 8.4 simulation software [31]. According to Jones & Deneys (1998), the smelting

temperature for typical Cu slags can be estimated to be 1500 °C [32]. The main reactions and standard Gibbs free energies (ΔG°) per mole of reductant (CO or C) are as follows:

$$C_{(s)} + CO_{2(g)} = 2CO_{(g)} \quad (1)$$

$$\Delta G^0_{(1500\ ^\circ C)} = -32.793\ \text{kcal mol}^{-1}$$

$$Cu_2O_{(l)} + CO_{(g)} = 2Cu_{(l)} + CO_{2(g)} \quad (2)$$

$$\Delta G^0_{(1500\ ^\circ C)} = -20.310\ \text{kcal mol}^{-1}$$

$$PbO_{(l)} + CO_{(g)} = Pb_{(l)} + CO_{2(g)} \quad (3)$$

$$\Delta G^0_{(1500\ ^\circ C)} = -16.522\ \text{kcal mol}^{-1}$$

$$CoO_{(s)} + CO_{(g)} = Co_{(l)} + CO_{2(g)} \quad (4)$$

$$\Delta G^0_{(1500\ ^\circ C)} = -4.823\ \text{kcal mol}^{-1}$$

$$FeO_{(l)} + CO_{(g)} = Fe_{(s)} + CO_{2(g)} \quad (5)$$

$$\Delta G^0_{(1500\ ^\circ C)} = 5.548\ \text{kcal mol}^{-1}$$

$$FeO_{(l)} + C_{(s)} = Fe_{(s)} + CO_{(g)} \quad (6)$$

$$\Delta G^0_{(1500\ ^\circ C)} = -27.244\ \text{kcal mol}^{-1}$$

$$ZnO_{(s)} + CO_{(g)} = Zn_{(g)} + CO_{2(g)} \quad (7)$$

$$\Delta G^0_{(1500\ ^\circ C)} = -4.803\ \text{kcal mol}^{-1}$$

$$1/3Ga_2O_{3(s)} + CO_{(g)} = 2/3Ga_{(l)} + CO_{2(g)} \quad (8)$$

$$\Delta G^0_{(1500\ ^\circ C)} = 9.915\ \text{kcal mol}^{-1}$$

$$1/3Ga_2O_{3(g)} + C_{(g)} = 2/3Ga_{(l)} + CO \quad (9)$$

$$\Delta G^0_{(1500\ ^\circ C)} = -22.878\ \text{kcal mol}^{-1}$$

$$1/2GeO_{2(g)} + CO_{(g)} = 1/2Ge_{(l)} + CO_{2(g)} \quad (10)$$

$$\Delta G^0_{(1500\ ^\circ C)} = -1.947\ \text{kcal mol}^{-1}$$

The ability of metal oxides to be reduced by carbon and CO, as well as the order of the carbothermic reduction reactions, can be estimated using Ellingham phase diagrams [33]. Ellingham phase diagrams for the oxidation of different TMs and BMs contained in Cu slag were generated using FactSage 8.4 thermochemical software and are presented in Figure 1 [31]. The Ellingham diagrams show that CO formation is enhanced by an increase in temperature, whereas metal oxides become increasingly unstable. This favours the carbothermic reduction in metal oxides, in which the Gibbs free energy of formation is higher than that of CO formation [33]. The diagrams also show that the carbothermic reduction in the technology and base metal oxides of interest co-occurs with that of FeO, resulting in an iron-based alloy, considering that the Cu slag has high FeO contents. The co-metallisation of TMs, BMs, and Fe increases the alloy mass collection and has the adverse effect of diluting the TM and BM contents in the final alloy.

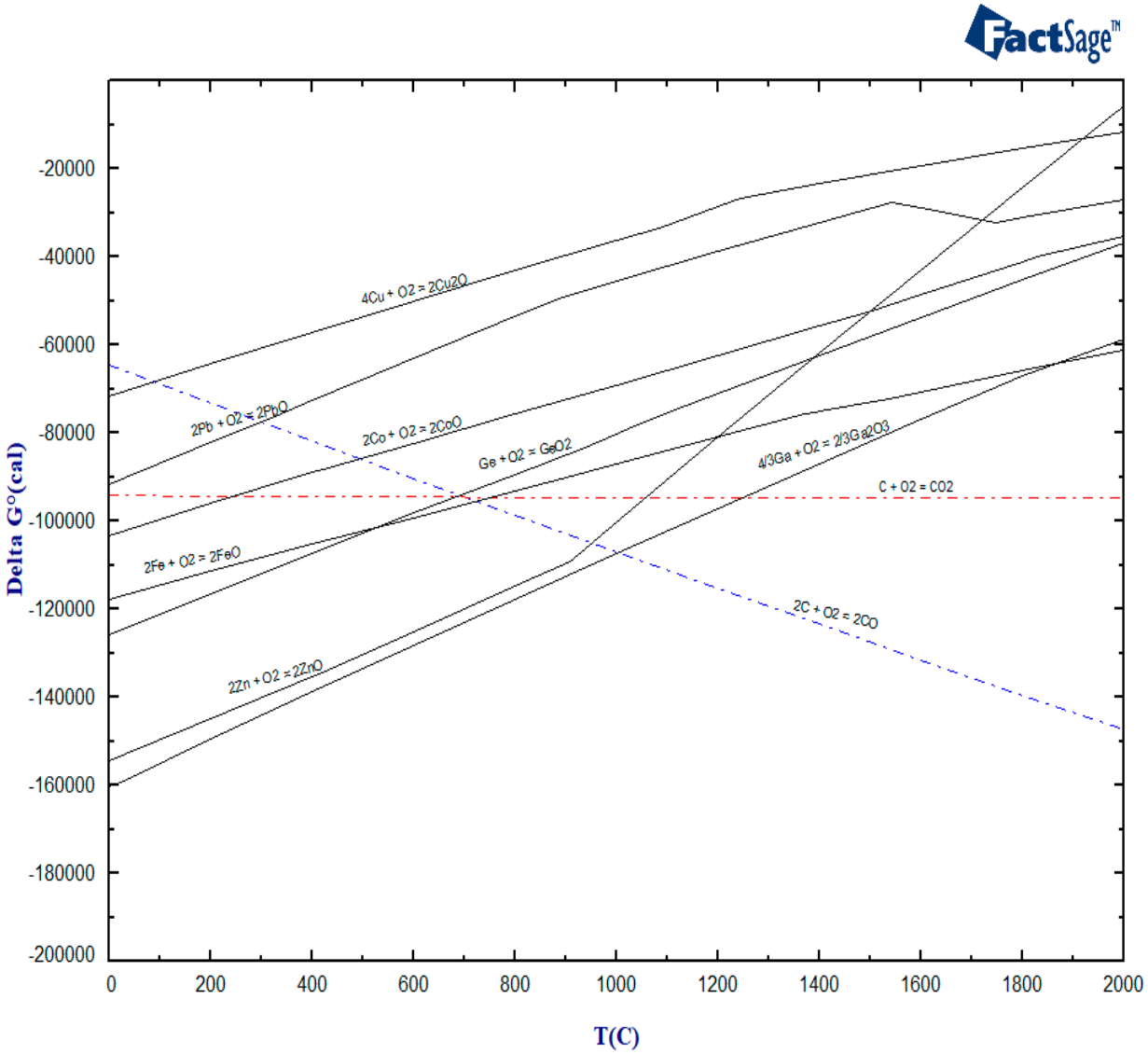


Figure 1. Standard Gibbs free energy for metal oxides of interest in Cu slag.

FactSage software was used to generate temperature phase stability diagrams for the TMs and BMs under low pO_2 applicable in carbothermic smelting of Cu slags at 1 atm, as shown in Figure 2. In carbothermic reduction and smelting, the relationship between pO_2 and pCO/pCO_2 is defined by chemical reaction (11) [34]. These results show that carbothermic smelting of copper slags for the extraction of the targeted TMs and BMs requires low pO_2, i.e., a higher pCO/pCO_2 volume ratio, with Ga and Zn metallisation requiring the lowest pO_2 of $<10^{-10}$ atm at the indicative smelting temperature of 1500 °C [32].

$$CO + 1/2O_2 = CO_2 \quad (11)$$

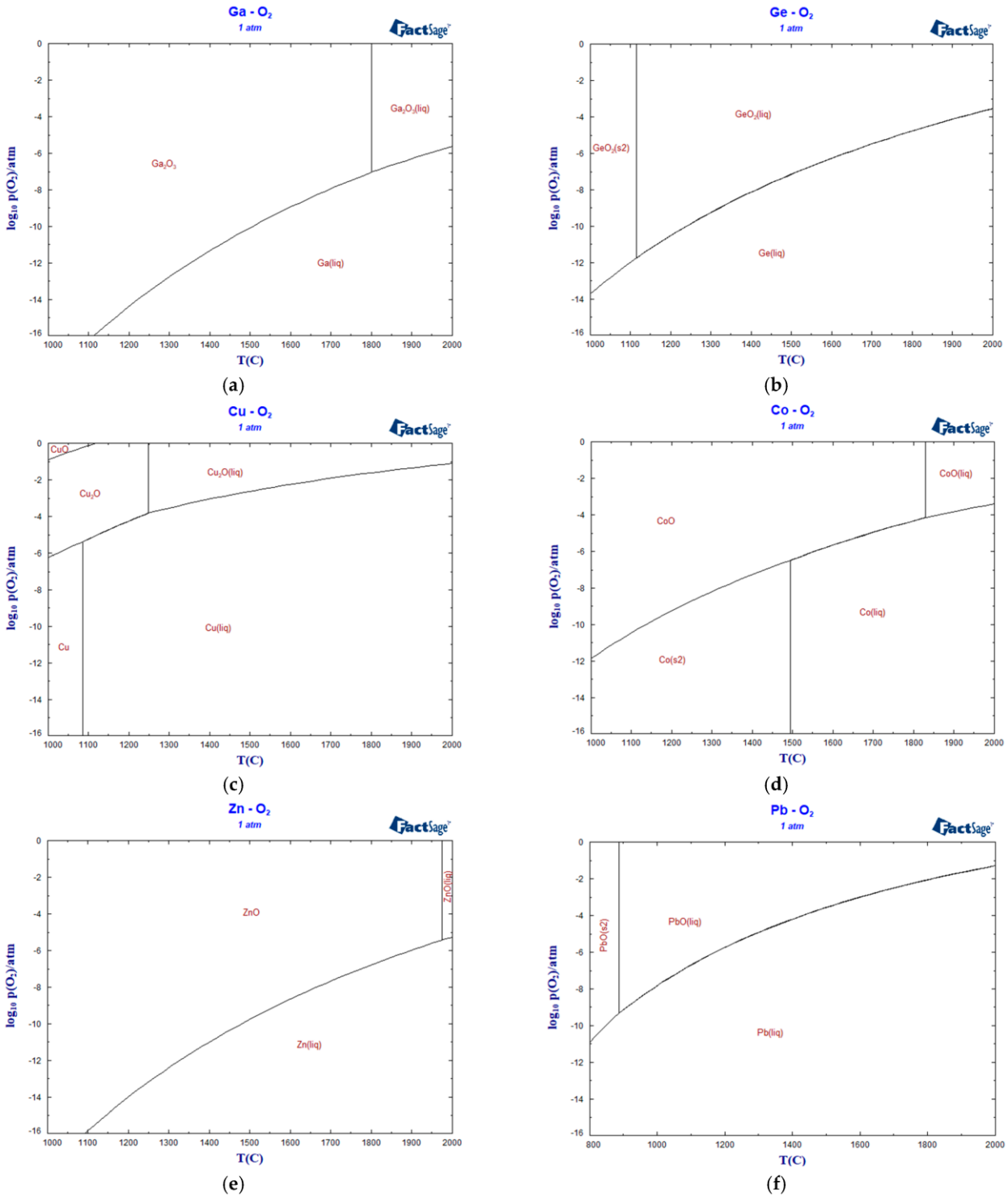


Figure 2. Phase stability diagrams under low pO_2 applicable in carbothermic smelting of Cu slags at 1 atm for the systems: (**a**) Ga-O_2, (**b**) Ge-O_2, (**c**) Cu-O_2, (**d**) Co-O_2, (**e**) Zn-O_2, and (**f**) Pb-O_2.

2. Experiments

2.1. Materials and Equipment

Cu slag obtained from a slag dump site in Lubumbashi in the DRC was used in the current study. High-grade graphite (99.99% C), supplied by Merck (Darmstadt, Germany), was used as a reductant. High-purity alumina crucibles used in the smelting tests were supplied by Engchem (Pty) Ltd. (Randvaal, South Africa). The graphite susceptor was supplied by GrafTech International Ltd. (Brooklyn Heights, OH, USA).

Smelting tests were conducted using a 25 kW induction furnace supplied by LH Power Electronics (Pty) Ltd., now known as Keegor Group (Pty) Ltd. (Benoni, South Africa). A schematic of the induction furnace setup is shown in Figure 3. The experimental setup utilised a castable alumina (>97% Al_2O_3) crucible, with 28.0 cm outside diameter (OD), 24.0 cm inside diameter (ID), and an external height of 43.0 cm, centred inside the copper induction coils. A 5 cm thick layer of coarse alumina bubbles, with 2–3 mm particle size, was packed inside the castable alumina crucible. The graphite susceptor crucible, with 18.0 cm OD, 15 cm ID and a 30.0 cm height, including the lid, was placed on the layer of the alumina bubbles. More alumina bubbles were poured around the graphite crucible for thermal insulation. Another 5 cm thick layer of alumina bubbles was packed inside the graphite crucible. The tests were conducted in a 750 mL conical high-purity alumina (>99% Al_2O_3) crucible, with 11.1 cm top OD, 12.8 cm height, 7.0 cm bottom OD, and 0.6 cm wall thickness. The charged conical alumina crucible was placed on the layer of alumina bubbles inside the graphite crucible. The graphite crucible was closed with a three-hole lid, accommodating a gas inlet, a thermocouple, and an off-gas outlet.

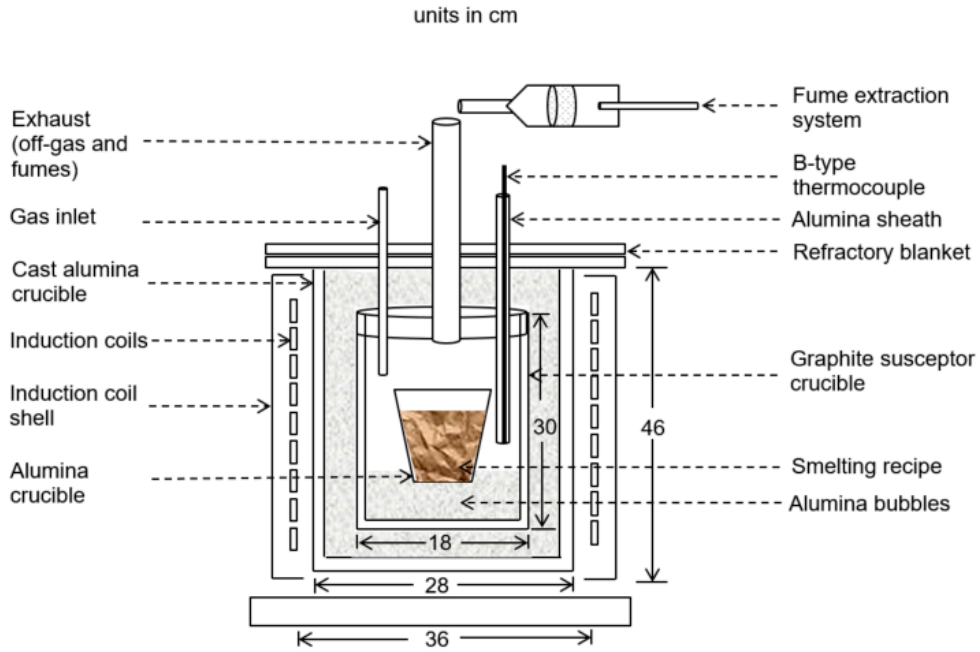


Figure 3. Schematic of the 25 kW induction furnace setup modified from Goso (2019) [34].

Argon gas was introduced into the system through a two-open-end alumina tube with 0.8 cm OD and 0.6 cm internal diameter (ID). Another alumina tube of the same size, but with one closed end, was used as a thermocouple protection sheath. A B-type thermocouple connected to a Keysight data acquisition unit was used for measuring the test temperature. More alumina bubbles and a refractory blanket were put on top of the closed graphite crucible for thermal insulation. A fume collection system, made up of a steel vessel with fume collection bags, was positioned about 3 cm above the 6 cm OD and 0.6 cm thick exhaust pipe to collect the fumes from the off-gas stream. Fume collection was not quantitative, as the system was not fully closed.

Chemical analyses of the test samples were conducted by the Agilent 5110 Synchronous Vertical Dual View inductively coupled plasma optical emission spectrometer (ICP–OES) (Santa Clara, CA, USA) operated by the ICP Expert v7.4.1 software, a Thermo Scientific iCAP Q inductively coupled plasma mass spectrometer (ICP-MS) (Waltham, MA, USA) operated by the Qtegra software version TEA 2.18 FR1, and a CS744 LECO instrument (St. Joseph, MI, USA).

The chemical composition of the Cu slag used in the study is presented in Table 1.

Table 1. Bulk composition of the Cu slag (mass %).

MgO	Al_2O_3	SiO_2	CaO	TiO_2	MnO	FeO	CoO	CuO	ZnO	PbO	Ga_2O_3 (ppm)	GeO_2 (ppm)
5.48	3.97	33.45	10.22	0.44	0.14	24.76	1.08	3.68	14.38	0.78	293	303

2.2. Thermochemical Simulations

Thermochemical simulations using FactSage 8.4 software were conducted to guide the subsequent experimental investigations for the secondary smelting of the Cu slag to extract TMs and BMs in an iron-based alloy. FactSage is a well-established commercial computer package used worldwide to calculate multi-component phase equilibria and determine smelting characteristics of different materials. This software is equipped with the world's largest set of evaluated and optimised thermodynamic databases for inorganic systems [31].

FactSage was used to simulate the smelting of the Cu slag for the extraction of TMs and BMs, with a particular focus on the carbonaceous reductant requirements and recovery efficiencies. Smelting was simulated at temperatures ranging from 1300 to 1600 °C, with varying carbon additions to the feed. The 'FactPS' database was used to account for the gaseous species and other pure substances, 'FTOxid' was used for the slag or oxide species, and 'SGTE' was used for the alloy phases. Calculations were performed using the 'Equilib' module, which operates using the Gibbs free energy minimisation principles to determine the distributions of chemical species between the equilibrium phases.

2.3. Experimental Investigations

Laboratory-scale smelting tests were conducted to investigate the recoveries of TMs (Ge and Ga) and BMs (Cu and Co) in an iron-based alloy from the Cu slag. Graphite was added as a reductant in amounts varying between 3% and 5% of the feed slag mass. The actual feed compositions are summarised in Table 2.

Table 2. Smelting feed recipes.

Test	Slag (g)	Graphite (g)	% Graphite to Slag
1A	301.2	9.3	3.09
1B	301.3	9.4	3.12
1C	301.4	9.2	3.05
2	300.8	12.3	4.09
3	300.5	15.4	5.12

Tests 1A–C are replicate tests.

Smelting recipes were prepared by mixing and blending the required amounts of feed slag and graphite. The respective mixtures were packed into conical alumina crucibles. Each charged crucible was placed in the induction furnace setup shown in Figure 2, and a continuous flow of Ar gas at 2 standard litres per minute was introduced to maintain an inert atmosphere around the test crucible throughout the test. The induction furnace was programmed to heat the sample at 10 °C/min to 1500 °C, remain at this temperature for 2 h, and then cool to ambient conditions under the same Ar flow.

For each test, the fumes, slag, and alloy were collected and analysed by ICP-OES and ICP-MS, as well as LECO for the determination of carbon content in the alloys. Recoveries of TMs and BMs in alloys and fumes (in the case of Zn) were calculated using Equation (12).

In the current context, recovery refers to the quantity of each TM and BM contained in the feed slag that is recovered in one of the product streams, i.e., fumes, slag, or alloy, after the smelting process.

$$\%\text{Recovery of element i} = \frac{M_i \text{ in a product stream}}{M_i \text{ in the feed}} \times 100 \quad (12)$$

where 'M_i' is the mass of element i.

3. Results and Discussion

3.1. Thermochemical Simulations

FactSage 8.4 does not have Ga modelled as an endmember in the 'Slag liq—all oxides + S' liquid solution thermodynamic database [31]. Thus, the calculated Ga distributions between the product streams, i.e., off-gas (and fumes), slag, and alloy, would be distorted.

3.1.1. Smelting Product Masses

Mass distributions of smelting products at temperatures of 1300–1600 °C with 3–6% carbon additions were calculated using FactSage and are presented graphically in Figure 4. The results show fairly consistent product mass distributions for a fixed carbon addition within the studied temperature range. Thus, product mass distributions were not significantly affected by the temperature variation in the reviewed range. These results confirm that the 1500 °C smelting temperature established by Jones and Deneys (1998) is appropriate for the current study.

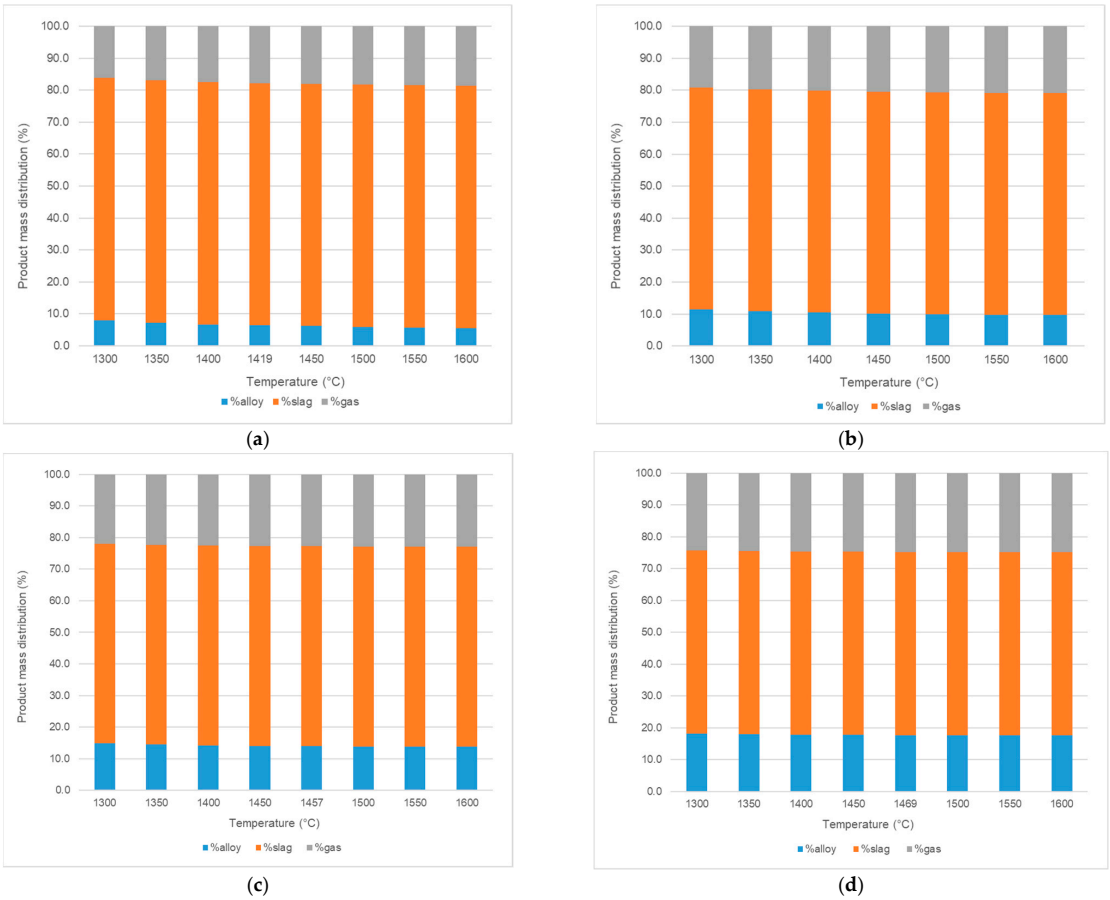


Figure 4. Calculated product mass distributions for smelting tests conducted at 1300–1600 °C with carbon additions of (**a**) 3%, (**b**) 4%, (**c**) 5%, and (**d**) 6%.

A comparison between the graphs in Figure 4 shows that the product mass distributions could be sensitive to carbon addition. The dependence of the product mass distributions on carbon addition was explored further at 1500 °C (experimental smelting temperature adopted from Jones and Deneys, 1998), and the result is shown in Figure 5. Carbon addition was increased up to 10% of the feed to evaluate the effectiveness of the carbothermic reaction. The masses of gas and alloy products increased with increasing carbon addition up to about 9.8% carbon addition. Thus, the smelting of the Cu slag at 1500 °C is sensitive to carbon addition in the tested range. Increments in gas and alloy product masses were attributed to the reduction in oxides and the formation of Zn fumes, the metallisation of Fe, Cu, Co, Ge, and Ga, and the formation of CO/CO_2 gas as the reduction reactions proceeded.

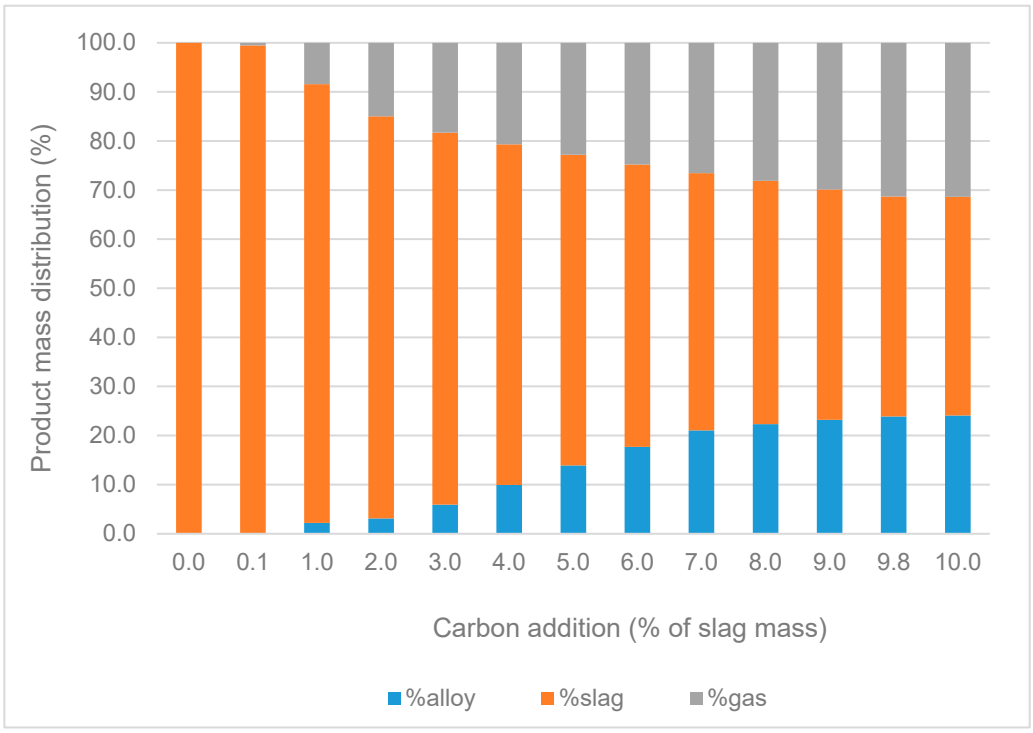


Figure 5. Distribution of calculated product masses as a function of carbon addition at 1500 °C.

3.1.2. Chemical Compositions of Products

Chemical compositions of the smelting products calculated at 1500 °C with carbon additions of up to 10% are presented in Table 3. Carbon addition of 9.8% to the feed slag marked the transition point from a complete liquid system to the solidification of face-centred-cubic (FCC) alloy crystals. Smelting with 9.8% carbon addition or more would be under sub-liquidus conditions; thus, the melt can be viscous, adversely affecting the separation efficiency of the alloy and slag and the tapping efficiency of the products.

Chemical compositions of solid fumes were deduced from the overall gas compositions by disregarding the concentrations of carbonaceous species (CO/CO_2). The results show that the fumes primarily comprised ZnO, formed from the oxidation of Zn metal fumes, and, to a lesser extent, PbO and CuO at trace concentration levels. The calculated compositions of the fumes were consistent.

Table 3. Measured chemical compositions of the smelting products (mass %).

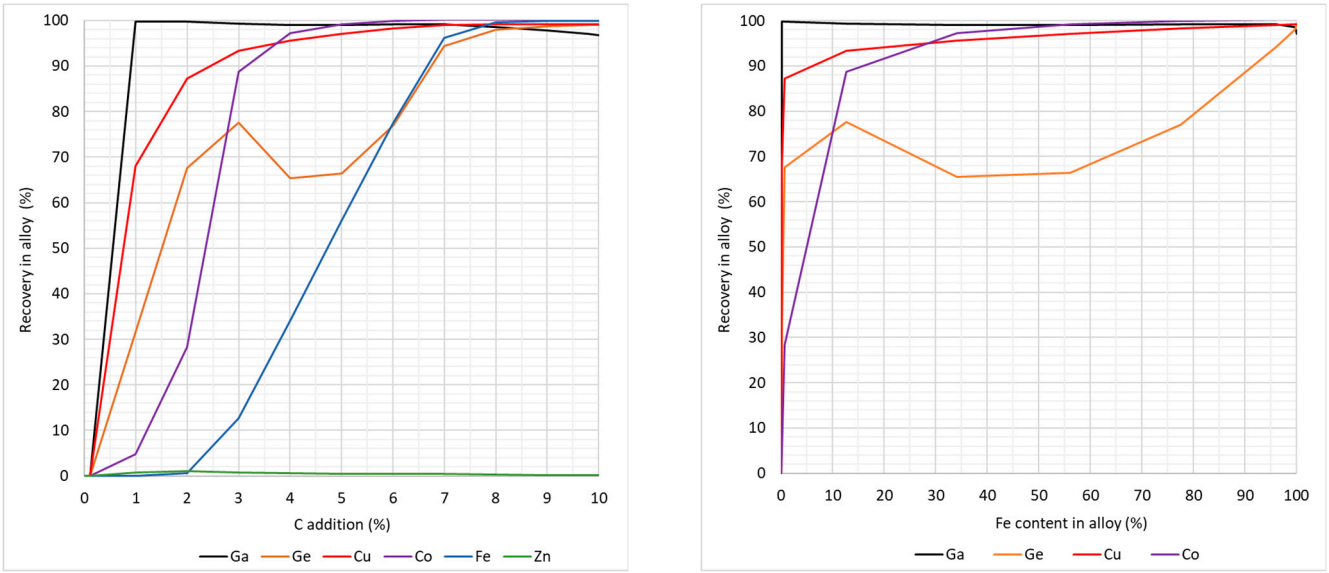
C Addition, %	MgO	Al_2O_3	SiO_2	CaO	TiO_2	MnO	FeO	CoO	CuO	ZnO	PbO	Ga_2O_3 (ppm)	GeO_2 (ppm)	C
Chemical compositions of fumes (normalised after excluding CO/CO_2) —concentrations of other components <0.01 mass%														
2.0	-	-	-	-	-	-	-	-	0.06	94.88	4.97	-	-	-
4.0	-	-	-	-	-	-	-	-	0.08	94.69	5.15	-	-	-
6.0	-	-	-	-	-	-	-	-	0.09	94.73	5.12	-	-	-
8.0	-	-	-	-	-	-	-	-	0.13	94.61	5.13	-	-	-
9.8	-	-	-	-	-	-	-	-	0.17	94.18	5.10	-	-	-
10.0	-	-	-	-	-	-	-	-	0.16	94.16	5.10	-	-	-
Chemical compositions of the slags —content of other components <0.01 mass%, Ga_2O_3 and GeO_2 < 1 ppm														
2.0	6.56	6.62	40.04	12.23	0.53	0.17	29.44	0.93	0.55	2.89	0.08	-	0.72	-
4.0	7.59	7.66	46.34	14.16	0.61	0.19	22.59	0.05	0.21	0.60	0.02	-	0.10	-
6.0	8.99	9.07	54.86	16.76	0.72	0.23	9.13	0.01	0.08	0.14	0.01	-	0.01	-
8.0	10.24	10.33	59.11	19.09	0.82	0.22	0.20	-	0.01	-	-	-	-	-
9.8	11.14	11.24	55.93	20.78	0.80	0.12	0.02	-	0.01	-	-	-	-	-
10.0	11.18	11.28	55.86	20.86	0.73	0.12	0.02	-	0.01	-	-	-	-	-
Chemical compositions of the alloys —contents of Mg, Al, Ca < 0.01%														
	Mg	Al	Si	Ca	Ti	Mn	Fe	Co	Cu	Zn	Pb	Ga	Ge	C
2.0	-	-	-	-	-	-	3.97	7.58	80.93	3.67	2.71	0.69	0.45	-
4.0	-	-	-	-	-	-	63.71	7.98	27.24	0.64	0.08	0.21	0.13	0.01
6.0	-	-	0.01	-	-	-	79.50	4.51	15.40	0.31	0.02	0.12	0.09	0.05
8.0	-	-	3.48	-	-	0.06	79.50	3.52	12.10	0.14	0.01	0.09	0.09	0.99
9.8	-	-	10.45	-	0.10	0.24	73.32	3.24	11.11	0.07	0.01	0.08	0.08	1.30
10.0	-	-	10.59	-	0.19	0.22	72.68	3.21	11.02	0.06	0.01	0.08	0.08	1.84

The FeO, CoO, CuO, ZnO, PbO, and GeO_2 contents in the slags decreased with increasing carbon addition in the feed until the identified transition point, where these chemical species were almost undetectable in the slag. The decreases in the contents of FeO and the oxides of the TMs and BMs of interest in the product slags were attributed to the reduction in the respective metal oxides to form alloys and fumes. These results are consistent with the results reported in the open literature [29,30].

Alloy chemical compositions show that the Fe, Si, and carbon contents increased with increasing carbon addition in the feed. In contrast, the contents of the elements of interest in the alloys decreased with increasing carbon addition. This behaviour was attributed to the dilution of TM and BM contents by Fe, Si, and C in the alloy. Although the metallisation of Fe is sensibly required to facilitate the mass collection of the alloy, high metallisation of Si and dissolution of carbon in the alloy are generally indicative of excessive reducing conditions. Hence, when smelting at 1500 °C, no more than 6% carbon should be added to the feed slag. A metallisation degree of 5–15%, which is equivalent to a maximum of 5% carbon addition to the feed slag (as shown in Figure 4), would suffice for effective separation and collection of the TM/BM-bearing alloy.

3.1.3. Calculated Metal Recoveries

Data from FactSage simulations were used to calculate the % recovery of Fe, TMs, and BMs in the alloy product at 1500 °C. Metal recoveries in the alloy are graphically presented as a function of carbon addition in Figure 6a. Recoveries of Ga, Ge, Cu, Co, and Fe increased with increasing carbon addition in the feed. Ge recovery increased up to a carbon addition of 3% in the feed. Complete recovery of Ga in the alloy with only 1% carbon addition in the feed is uncertain, considering the identified limitation of FactSage 8.4 in predicting Ga dissolution in the main slag liquid solution. The software predicted that Ga and Ge mainly partitioned between the off-gas and alloy streams. Zn recovery in the alloy was generally low due to the low fuming temperature of Zn metal at 907 °C.



(**a**) (**b**)

Figure 6. Recoveries of TMs and BMs in alloy at 1500 °C as a function of (**a**) carbon addition to feed slag, and (**b**) Fe content in the alloy.

For the practical extraction of TMs and BMs mainly in the alloy and Zn in the fumes, the extent of carbothermic reaction should target a minimum Fe recovery. The calculated recoveries of TMs and BMs in the alloy at 1500 °C are presented graphically as a function of Fe content in the alloy in Figure 6b. Recoveries of TMs and BMs generally increased with Fe content in the alloy. In line with the observed effect of carbon addition, Ge recovery in the alloy decreased between Fe contents of about 40 and 63 mass% in the slag. These operating conditions, involving acid slag, high operating temperatures, and low oxygen partial pressures, promoted a low Ge recovery in the slag. Similar trends were reported by Jones and Deneys (1998) for Co recovery from a similar slag. In addition, they reported that the liquid–liquid interchange reactions between the metal oxides (MO) in the slag and metals [M] in the alloy were significant, according to chemical reaction (13).

$$(MO) + [Fe] = [M] + (FeO) \quad (13)$$

Thermochemical simulation results showed that for the extraction of TMs and BMs from the studied Cu slag, carbothermic smelting at 1500 °C with a carbon addition of 3% or 4% in the feed slag mass is recommended. A carbon addition of 3% resulted in high recoveries of TMs and BMs in the alloy and Zn in the fumes, but the alloy mass collection was low, less than 10%. A carbon addition of 4% resulted in high Co and Cu recoveries in the alloy; however, Ge recovery dropped slightly for carbon additions of 3% and 4%. Lower

Ge recoveries could be attributed to some Ge deporting into the off-gas/fume stream or remaining in the slag, possibly due to the difficulty of reducing GeO_2, even under low pO_2.

3.2. Experimental Investigations

3.2.1. Smelting Product Masses

After smelting at 1500 °C, the slag and alloy were generally well separated. Mass distributions of alloy, slag, and fumes are plotted as a function of carbon addition in the feed in Figure 7. Statistical evaluation of product masses of test 1, conducted in triplicate, showed that the smelting procedure was repeatable. The mass percentages of off-gas, slag, and alloy were characterised by low coefficients of variation of 2.5%, 0.6%, and 4.2%, respectively, which confirmed the stability and consistency of test 1 repeats. In agreement with the simulation results, the masses of the off-gas and alloy increased with carbon addition in the feed slag. The results are consistent with expectations from thermodynamic considerations [33], namely, that increasing carbon addition translates to a greater reduction in TM and BM oxides from the slag.

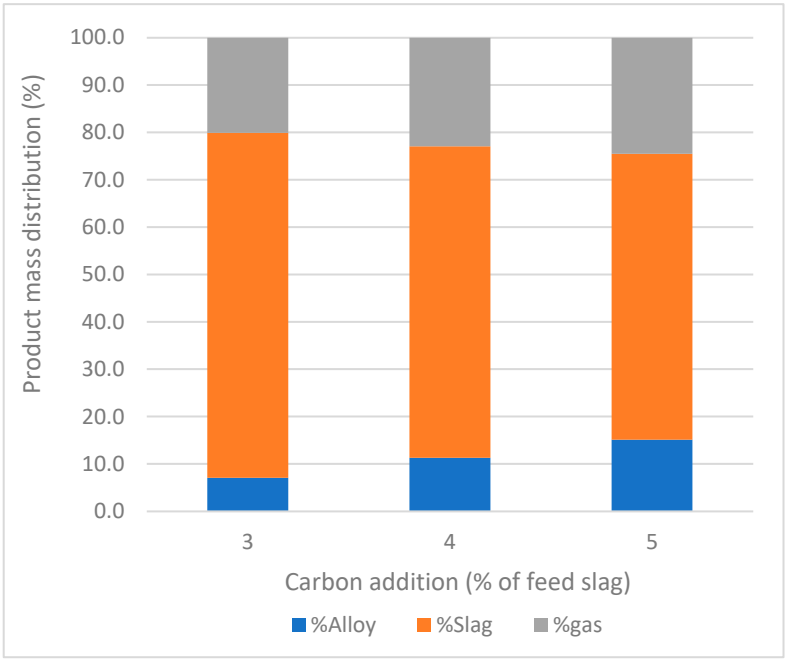


Figure 7. Mass distributions of alloy, slag, and off-gas with 3%, 4%, and 5% carbon additions at 1500 °C.

3.2.2. Chemical Compositions of Smelting Products

Chemical compositions of the smelting products produced at 1500 °C with carbon additions of 3% to 5% of the feed slag mass are presented in Table 4. Low standard deviations, except for Ga and Ge as well as other minor elements, confirmed that the replicate tests were reproducible. The relatively poor precision in the results of Ga, Ge, and other minor elements was attributed to measurement uncertainty.

The experimental chemical analysis results agree with the simulation results, showing that the fumes primarily comprised ZnO and, to a lesser extent, PbO. FeO content in the slag decreased with increasing carbon addition in the feed, indicating that more Fe was reduced to the alloy as more carbon was added to the feed. The alloy primarily comprised Fe, with significant contents of BMs such as Co and Cu, as well as TMs such as Ga and Ge. Fe content in the alloy increased with increasing carbon addition in the feed. Thus, efforts to scale up the proposed process should target carbon additions that result in the lowest Fe content in the alloy, corresponding to the maximum extraction efficiencies of TMs and BMs.

Table 4. Measured chemical compositions of the smelting products (mass %).

Test	MgO	Al_2O_3	SiO_2	CaO	TiO_2	MnO	FeO	CoO	CuO	ZnO	PbO	Ga_2O_3 (ppm)	GeO_2 (ppm)	C
Chemical compositions of the fumes														
1A	0.89	0.54	1.27	0.44	<0.05	<0.05	0.96	<0.05	0.58	88.1	7.23	90.52	32.11	
1B	0.27	0.93	0.56	0.64	<0.05	<0.05	<0.05	<0.05	0.81	88.1	8.71	164.88	49.50	
1C	<0.05	0.17	0.51	0.27	<0.05	<0.05	<0.05	<0.05	0.20	90.7	8.13	71.96	14.60	
Mean	0.58	0.55	0.78	0.45	<0.05	<0.05	0.96	<0.05	0.53	88.97	8.02	109.12	32.07	
Stdev	0.44	0.38	0.43	0.19	0.00	0.00	0.00	0.00	0.31	1.50	0.75	49.17	17.45	
2	<0.05	0.13	0.60	0.20	<0.05	<0.05	<0.05	<0.05	0.11	88.9	10.10	35.29	8.30	
3	<0.05	1.19	2.93	1.09	<0.05	<0.05	<0.05	0.22	0.84	87.5	6.18	30.25	24.50	
Chemical compositions of the slags														
1A	7.56	8.73	41.3	13.6	0.52	0.14	24.6	0.08	0.19	0.22	<0.05	38.31	19.74	
1B	7.01	8.62	46.2	14.4	0.57	0.15	25.0	0.10	0.16	0.14	<0.05	55.79	20.46	
1C	7.53	9.07	47.2	14.0	0.57	0.15	24.2	0.09	0.12	0.11	<0.05	44.76	23.48	
Mean	4.44	4.66	20.98	10.00	0.33	0.12	19.11	0.07	0.13	0.13	<0.05	34.43	14.73	
Stdev	0.19	0.12	1.47	0.30	0.02	0.01	0.29	0.01	0.03	0.05	0.00	6.57	1.38	
2	7.93	8.92	46.2	15.7	0.58	0.15	19.8	<0.05	0.12	0.22	<0.05	35.22	5.04	
3	9.72	10.49	55.4	18.6	0.68	0.18	8.26	<0.05	0.18	0.11	<0.05	40.46	23.05	
Chemical compositions of the alloys														
	Mg	Al	Si	Ca	Ti	Mn	Fe	Co	Cu	Zn	Pb	Ga	Ge	C
1A	<0.05	0.08	0.42	0.50	<0.05	<0.05	53.55	10.30	38.11	<0.05	<0.05	0.13	0.20	0.10
1B	<0.05	0.06	0.38	0.42	<0.05	<0.05	54.80	9.60	35.40	<0.05	<0.05	0.15	0.17	0.10
1C	<0.05	0.06	0.39	0.41	<0.05	<0.05	54.12	9.61	36.80	<0.05	<0.05	0.13	0.19	0.10
Mean	<0.05	0.07	0.40	0.44	<0.05	<0.05	54.16	9.84	36.77	<0.05	<0.05	0.14	0.19	0.10
Stdev	0.05	0.01	0.02	0.05	0.05	0.05	0.63	0.40	1.36	0.05	0.05	0.01	0.02	0.00
2	<0.05	0.06	0.28	0.43	<0.05	<0.05	70.50	6.62	23.60	<0.05	<0.05	0.11	0.13	0.18
3	<0.05	0.08	0.34	0.45	<0.05	<0.05	78.80	4.88	17.45	<0.05	<0.05	0.08	0.10	0.36

<0.05 mass% analyte content below the limit of detection.

3.2.3. Metal Recoveries

Recoveries of Fe, TMs, and BMs in the alloy after smelting at 1500 °C are presented in Figure 8 as a function of carbon addition in the feed slag. Recoveries of Ga, Ge, Cu, Co, and Fe generally increased with increasing carbon addition in the feed. At 3% carbon addition, recoveries of TMs and BMs could still be increased. However, at 4–5% carbon additions, these recoveries somewhat plateaued, suggesting that 4% carbon addition in the feed should be considered the best amount to reduce Fe recovery and thus limit the dilution of the TMs and BMs in the alloy. These results generally agree with results in the literature [29,30].

At 4% carbon addition in the feed, the respective recoveries of Co and Cu were 91% and 94%, while those of Ga and Ge were about 50% and 70%. In future work, a basic oxide, such as CaO or MgO, could be added to the feed to flux the secondary slag and maximise the recoveries of these TMs and BMs. Furthermore, varying the smelting temperature would elucidate its impact on the extraction efficiencies of TMs and BMs from the Cu slag, which is critical for maximising metal recovery. High temperatures typically enhance reduction reactions in the feed slag and improve the separation of the alloy and secondary slag [35]. Zn and Pb were primarily recovered in the fume stream, with efficiencies of over 90%.

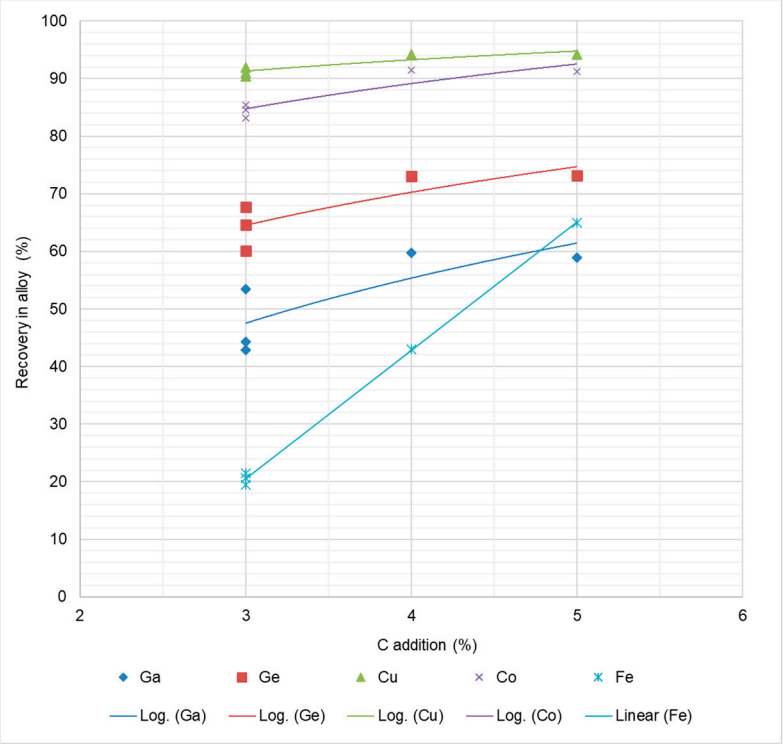


Figure 8. Recoveries of Fe, TMs, and BMs in alloy at 1500 °C.

Table 5 compares TM and BM recoveries in the alloy based on FactSage simulation and experimental results. The percentage difference (%Diff) was calculated as the absolute value of the percentage change in value, divided by the average of the experimental and FactSage calculated data, for comparison purposes. Recoveries of Ga, Ge, Cu, and Co in the alloy were higher in thermochemical simulations than in experiments, likely because simulations assume thermodynamic equilibrium, whereas the experiments were subject to kinetic and mass transfer constraints. FactSage predicted near-total Ga recoveries in the alloys. However, these results showed the largest %Diff from experimental data, due to the lack of a suitable thermodynamic database for the liquid slag phase. Experimental Ge recoveries in the alloys were low, indicating a significant Ge deportment to the off-gas and/or slag. FactSage and experimental Cu and Cu recoveries in alloys had a lower %Diff of <10%, indicating a lower impact of kinetic and mass transfer constraints in these experimental results.

Table 5. Comparison of TM and BM recoveries in alloy, based on FactSage simulation and experimental results (%).

	Carbon Addition, %	**3 ***		**4**		**5**	
	Parameters	**%**	**%Diff**	**%**	**%Diff**	**%**	**%Diff**
Ga	FactSage calculation Experiments	99.28 46.88	71.7	98.98 59.78	49.4	99.05 58.94	50.8
Ge	FactSage calculation Experiments	77.63 64.13	19.0	65.44 73.05	11.0	66.44 73.13	9.6
Co	FactSage calculation Experiments	88.67 84.40	4.9	97.18 91.48	6.0	99.12 91.20	8.3
Cu	FactSage calculation Experiments	93.35 91.16	2.4	95.53 94.23	1.4	97.08 94.23	3.0

* Average of three experimental results.

4. Conclusions

FactSage thermochemical simulations and induction furnace smelting experiments were conducted to investigate the technical feasibility of carbothermic smelting for extracting TMs and BMs from Cu slag. Ga, Ge, Co, and Cu were primarily recovered in an iron-based alloy, while Zn and Pb oxidised to ZnO and PbO fumes. Simulation results showed that the alloy mass increased with increasing carbon addition in the feed but was less sensitive to variation in smelting temperature between 1300 and 1600 °C. The TM and BM contents in the alloy decreased with increasing carbon addition in the feed due to dilution, mainly by Fe. A satisfactory alloy comprising about 70.5% Fe, 6.6% Co, 23.6% Cu, 0.11% Ga, and 0.13% Ge was produced when smelting at 1500 °C with 4% carbon addition in the feed. The associated recovery rates were over 90% for Co and Cu, over 50% for Ga, and over 70% for Ge. Zn and Pb were primarily collected in the fumes, each with over 90% recovery. Further work is recommended to investigate the feasibility of using conventional hydrometallurgical flowsheets for the separation and production of high-purity TMs and BMs. However, high-Fe content in the feed alloy will likely increase reagent consumption and costs, complicating the hydrometallurgical separation and refining of TMs and BMs. Techno-economic and environmental assessments of the overall process flowsheets must also be conducted.

Author Contributions: Conceptualisation, X.C.G. and M.K.; methodology, K.G.S., K.C.M. and X.C.G.; software, X.C.G., K.G.S., A.N., K.C.M. and M.K.; validation, X.C.G., A.N. and M.K.; formal analysis, K.G.S., A.N. and K.C.M.; investigation, X.C.G., K.G.S., A.N., K.C.M. and M.K.; resources, X.C.G. and M.K.; data curation, X.C.G., K.G.S., A.N., K.C.M. and M.K.; writing—original draft preparation, X.C.G., K.C.M. and M.K.; writing—review and editing, X.C.G., K.G.S., A.N., K.C.M. and M.K.; visualisation, K.G.S. and K.C.M.; supervision, X.C.G., A.N. and M.K.; project administration, X.C.G.; funding acquisition, X.C.G. All authors have read and agreed to the published version of the manuscript.

Funding: This research was funded by Mintek, grant number State Grant GaGeProject (PDR-00024019).

Data Availability Statement: The data presented in this study are available on request from the corresponding author. The data are not publicly available due to restrictions imposed by the funding company.

Acknowledgments: The paper is published with the permission of Mintek.

Conflicts of Interest: Authors Xolisa Camagu Goso and Kgothatso Gerald Sethosa were employed by the company Pyrometallurgy Division, Mintek. Author Kgomotso Charlotte Maluleke was employed by the company Tenova Pyromet, Tenova South Africa (Pty) Ltd. The remaining authors declare that the research was conducted in the absence of any commercial or financial relationships that could be construed as a potential conflict of interest.

Abbreviations

The following abbreviations are used in this manuscript:

TMs	Technology Metals
BMs	Base Metals
DRC	Democratic Republic of Congo
LEDs	Light-emitting diodes
ICP-OES	Inductively Coupled Plasma Optical Emission Spectroscopy
ICP-MS	Inductively Coupled Plasma Mass Spectrometry

References

1. Singer, D.A.; Berger, V.I.; Moring, B.C. *Porphyry Copper Deposits of the World: Database and Grade and Tonnage Models*; U.S. Geological Survey: Reston, VA, USA, 2008.
2. Jones, R.T.; Mackey, P.J. An Overview of Copper Smelting in Southern Africa. *Copp. Cobalt Afr.* **2015**, *2*, 499–504.
3. Nordbrand, S.; Bolme, P. *Powering the World: Cobalt production for Batteries in the DR Congo and Zambia*; SwedWatch: Stockholm, Sweden, 2007.
4. Schlechten, A.W.; Taylor, J.C.; Butts, A. Copper Processing. 2017. Available online: https://www.britannica.com/technology/copper-processing (accessed on 18 June 2022).
5. Kojo, I.V.; Huppe, H. Sustainable copper production processes from mine to cathode copper: Some process selection considerations. In Proceedings of the Conference on Clean Technologies for the Mining Industry, Santiago, Chile, 10–12 April 2011.
6. Nikoloski, A.; Singh, P.; Chanda-Phiri, T. An overview of global copper smelting slag production and reprocessing approaches. In Proceedings of the XVI International Mineral Processing and Recycling Conference, Belgrade, Serbia, 28–30 May 2025.
7. Kasemodel, M.C.; Papa, T.B.; Sigolo, J.B.; Rodrigues, V.G. Assessment of the mobility, bioaccessibility, and ecological risk of Pb and Zn on a dirt road located in a former mining area—Ribeira Valley—Brazil. *Environ. Monit. Assess.* **2019**, *191*, 101. [CrossRef]
8. Ettler, V. Soil contamination near non-ferrous metal smelters: A review. *Appl. Geochem.* **2016**, *64*, 56–74. [CrossRef]
9. Mitrašinović, M.; Yuankun, Y.; Stopic, S.; Radosavljević, M. Feasibility of Recovering Valuable and Toxic Metals from Copper Slag Using Iron-Containing Additives. *Metals* **2023**, *13*, 1467. [CrossRef]
10. Latunussa, C.E.; Georgitzikis, K.; de Matos, C.T.; Grohol, M.; Eynard, U.; Wittmer, D.; Mancini, L.; Unguru, M.; Pavel, C.; Carrara, S.; et al. *Study on the EU's List of Critical Raw Materials*; European Commission: Brussels, Belgium, 2020.
11. Jones, R.T.; Pawlik, C. Cobalt Recovery from Southern African Copper Smelters. In Proceedings of the 58th Annual Conference of Metallurgists (COM) Hosting the 10th International Copper Conference, Vancouver, BC, Canada, 8–21 August 2019.
12. Rankin, W.J.; Hayes, P.C. The mineralogy and structure of ferrous silicate slags. *Metall. Trans. B* **1993**, *24*, 103–109.
13. USGS. *Mineral Commodity Summaries (Copper, Nickel, Cobalt, Zinc, Lead)*; USGS: Reston, VA, USA, 2024.
14. European Commission. *Critical Raw Materials Act—Assessment Report*; European Commission: Brussels, Belgium, 2023.
15. Gorai, B.; Jana, R.K.; Premchand. Characteristics and utilisation of copper slag—A review. *Resour. Conserv. Recycl.* **2003**, *39*, 299–313. [CrossRef]
16. Mussapyrova, L.; Nadirov, R.; Balaz, P.; Rajnak, M.; Bures, R.; Balaz, M. Selective room-temperature leaching of copper from mechanically activated copper smelter slag. *J. Mater. Res. Technol.* **2021**, *12*, 2011–2025. [CrossRef]
17. Potysz, A.; Kierczak, J. Prospective (Bio)leaching of Historical Copper Slags as an Alternative to Their Disposal. *Minerals* **2019**, *9*, 542. [CrossRef]
18. Khalid, M.K.; Hamuyuni, J.; Agarwal, V.; Pihlasalo, J.; Haapalainen, M.; Lundstrom, M. Sulfuric acid leaching for capturing value from copper rich converter slag. *J. Clean. Prod.* **2019**, *215*, 1005–1013. [CrossRef]
19. Potysz, A.; van Hullenbusch, E.D.; Kierczak, J.; Grybos, M.; Lens, P.N.; Guibaud, G. Copper Metallurgical Slags—Current Knowledge and Fate: A Review. *Crit. Rev. Environ. Sci. Technol.* **2015**, *45*, 2424–2488. [CrossRef]
20. Zhang, Y.; Man, R.; Ni, W.; Wang, H. Selective Leaching of Base Metals from Copper Smelter Slag. *Hydrometallurgy* **2010**, *103*, 25–29. [CrossRef]
21. Banza, A.N.; Gock, E.; Kongolo, K. Base Metals Recovery from Copper Smelter Slag by Oxidising Leaching and Solvent Extraction. *Hydrometallurgy* **2002**, *67*, 63–69. [CrossRef]
22. Boyrazli, M.; Altundogan, H.S.; Tumen, F. Recovery of Metlas from Copper Converter Slag by Leaching with $K_2Cr_2O_7$-H_2SO_4. *Can. Metall. Q.* **2006**, *45*, 145–152. [CrossRef]
23. Ziyadanogullari, B. Recovery of Copper and Cobalt from Concentrate and Converter Slag. *Sep. Sci. Technol.* **2000**, *35*, 1963–1971. [CrossRef]
24. Hellstén, N.; Klemettinen, L.; Sukhomlinov, D.; O'Brien, H.; Taskinen, P. Slag Cleaning Equilibria in Iron Silicate Slag–Copper Systems. *J. Sustain. Metall.* **2019**, *5*, 463–473. [CrossRef]
25. Wang, J.P.; Hwang, K.M.; Choi, H.M. A Study on the Recovery of Iron from Copper Slag with Temperature. *Int. J. Appl. Eng. Res.* **2018**, *13*, 977–982.
26. Li, S.; Wu, Z.; Yang, L.; Zhou, X. Direct reduction of copper slag with H_2 and CO: Effects of $CaCO_3$ on reduction kinetics. *J. Taiwan Inst. Chem. Eng.* **2025**, *178*, 106371. [CrossRef]
27. Kyei, D.A.; Sukhomlinov, D.; Klemettinen, L.; Michallik, R.; O'Brien, H.; Taskinen, P.; Lindberg, D. Pyrometallurgical Reduction of Copper Slag with Biochar for Metal Recovery. *J. Sustain. Metall.* **2024**, *10*, 1170–1187. [CrossRef]
28. Zhang, B.; Zhang, T.; Dou, Z. A Thermodynamic and Experimental Assessment of the Recovery of Copper, Iron, Zinc, and Lead from Copper Slag. *Minerals* **2022**, *12*, 496. [CrossRef]
29. Palacios, J.; Sanchez, M. Wastes as resources: Update on recovery of valuable metals from copper slags. *Miner. Process. Extr. Metall.* **2011**, *120*, 218–224. [CrossRef]

30. Sarfo, P.; Wyss, G.; Ma, G.; Das, A.; Young, C. Carbothermal reduction of copper smelter slag for recycling into pig iron and glass. *Miner. Eng.* **2017**, *107*, 8–19. [CrossRef]
31. Bale, C.W.; Belisle, E.; Chartrand, P.; Decterov, S.A.; Eriksson, G.; Gheribi, A.E.; Hack, K.; Jung, I.-H.; Kang, Y.-B.; Melancon, J.; et al. FactSage thermochemical software and databases, 2010–2016. *CALPHAD Comput. Coupling Phase Diagr. Thermochem.* **2016**, *54*, 35–53.
32. Jones, R.T.; Deneys, A.C. Using a direct-current arc furnace to recover cobalt from slags. *J. Miner. Met. Mater. Soc.* **1998**, *50*, 57–61. [CrossRef]
33. Habashi, F. *Textbook of Pyrometallurgy*; Metallurgie Extractive Quebec: Quebec, QC, Canada, 2002.
34. Goso, X.C. Phase Equilibria Studies and Beneficiation of Titaniferous Slags. Ph.D. Thesis, University of Cape Town, Cape Town, South Africa, 2019.
35. Zhang, C.; Zhang, Y.; Zhang, Z.; Zhang, G. Effective separation and recovery of valuable metals from copper slag: A comprehensive review. *Environ. Res.* **2025**, *283*, 122145. [CrossRef]

Disclaimer/Publisher's Note: The statements, opinions and data contained in all publications are solely those of the individual author(s) and contributor(s) and not of MDPI and/or the editor(s). MDPI and/or the editor(s) disclaim responsibility for any injury to people or property resulting from any ideas, methods, instructions or products referred to in the content.